

Effects of local structural damage in a steel truss bridge on internal dynamic coupling and modal damping

Hiroki Yamaguchi¹, Yasunao Matsumoto^{*1} and Tsutomu Yoshioka²

¹*Department of Civil and Environmental Engineering, Saitama University
255 Shimo-Ohkubo, Sakura, Saitama 338-8570, Japan*

²*Nippon Engineering Consultants Co., Ltd, 3-23-1, Komagome, Toshima, Tokyo 170-0003, Japan*

(Received November 15, 2014, Revised February 15, 2015, Accepted February 18, 2015)

Abstract. Structural health monitoring of steel truss bridge based on changes in modal properties was investigated in this study. Vibration measurements with five sensors were conducted at an existing Warren truss bridge with partial fractures in diagonal members before and after an emergency repair work. Modal properties identified by the Eigensystem Realization Algorithm showed evidences of increases in modal damping due to the damage in diagonal member. In order to understand the dynamic behavior of the bridge and possible mechanism of those increases in modal damping, theoretical modal analysis was conducted with three dimensional frame models. It was found that vibrations of the main truss could be coupled internally with local vibrations of diagonal members and the degree of coupling could change with structural changes in diagonal members. Additional vibration measurements with fifteen sensors were then conducted so as to understand the consistency of those theoretical findings with the actual dynamic behavior. Modal properties experimentally identified showed that the damping change caused by the damage in diagonal member described above could have occurred in a diagonal-coupled mode. The results in this study imply that damages in diagonal members could be detected from changes in modal damping of diagonal-coupled modes.

Keywords: structural health monitoring; truss bridge; vibration measurement; ERA; diagonal member-coupled vibration; modal damping; damage detection

1. Introduction

A number of bridges constructed during the rapid economic growth period from 1950's are having aging problem in Japan. There were serious incidents due to deterioration or damage for steel truss bridges found in rigorous inspections conducted after the tragic bridge collapse in Minneapolis, USA (Fujino and Siringoringo 2008). In the current standard bridge management strategy in Japan, primary periodic inspections rely on visual inspection, although various nondestructive test methods have been used in second step detailed inspections (National guideline 2014). For visual inspection, decreases in the number of skilled engineers and the reliability in subjective method are current and future concerns. Recent accidents found in steel truss bridges imply some limitations of visual inspection. Diagnosis of bridges based on physical behaviors

*Corresponding author, Professor, E-mail: ymatsu@mail.saitama-u.ac.jp

through measurements of deformations, stresses, vibrations, and so on, is required.

Vibration-based structural health monitoring, SHM, has been considered as a complementary method to visual inspection and studied worldwide (Doebbling *et al.* 1996, Balageas *et al.* 2006, Boller *et al.* 2009). Practical applications of vibration monitoring to existing bridges have been made mainly to specific long span bridges (e.g., Ko and Ni 2005, Fujino and Siringoringo 2008). There have been studies that investigate the relationship between the dynamic characteristics and artificial damages in existing bridges (e.g., Kim and Stubbs (2003), Maeck and de Roeck (2003)).

For the application of vibration-based SHM to steel truss bridge to detect local damages, such as fatigue cracks, corrosion, and bolt loosening, a number of sensors may be required, which leads to trade-off between monitoring cost and ability of damage detection. It would be, therefore, worth to develop a method to detect damage or evaluate structural state with less number of sensors. For SHM with less number of sensors, complimentary theoretical consideration is necessary. Previous studies of the dynamic characteristics of truss bridges can be referred to understand the global dynamic characteristics of truss bridges (e.g., Shama *et al.* 2001, Spyrakos *et al.* 2004), although there have not been studies of local vibration for damage detection in a local member to the authors' knowledge. In truss bridges, internal dynamic coupling between local vibration modes, such as bending of a member, and global vibration of the main truss can occur when their natural frequencies are close together. Similar coupling mechanism and its effect on modal damping have been reported for cable coupling vibration in a cable-stayed bridge (Yamaguchi *et al.* 2004).

The present study investigated SHM of steel truss bridges based on changes in modal properties, in particular, modal damping with internal dynamic coupling. Experimental and theoretical modal analyses were conducted for an existing truss bridge with partial fractures in diagonal members. Differences in natural frequency and modal damping identified before and after an emergency repair for diagonal members are discussed for possible application to SHM in this paper.

2. Effect of fracture in diagonal member on modal properties of truss bridge

2.1 Bridge studied

The bridge investigated was a bridge over a river for road traffic in-service from 1965. The bridge consisted of five separated spans, each of which was a simply supported Warren truss with a span length of 70.77 m and a width of 6.0 m (Fig. 1). The tension diagonal members had an H-section and the compression diagonal members had a box section, as shown in Figs. 1(c) and 1(d). There were eight or nine oval openings in the web of each tension diagonal members, except those at the ends of each span, for the reduction of the weight of steel (Fig. 2(a)).

During a visual inspection in July 2007 after 42-year service, partial fractures were found near the edge of gusset plate at either top or bottom end of longest tension diagonal members (D5 in Fig. 1), among which one in the fourth span resulted in loss of the half of its H-shaped cross section (Fig. 2(a)). In August 2007, as an emergency measure, additional steel plates with the same thickness as the member (i.e., 8 mm) were fixed by high strength bolts to cover both sides of the flanges and web for a length of about 1.5 m from the end of the members (Fig. 2(b)).

2.2 Vibration measurement

Vibration measurements were made at the fourth span in which the loss of half cross section

was found in D5. The measurements were conducted before and after the emergency repair in August 2007. Vibrations induced by a dump truck of 196 kN weight with three axles running over the bridge were recorded while there was no other traffic on the bridge. The dump truck ran in the traffic lane at the upstream side at a speed of 20, 30 or 40 km/h with three repetitions.

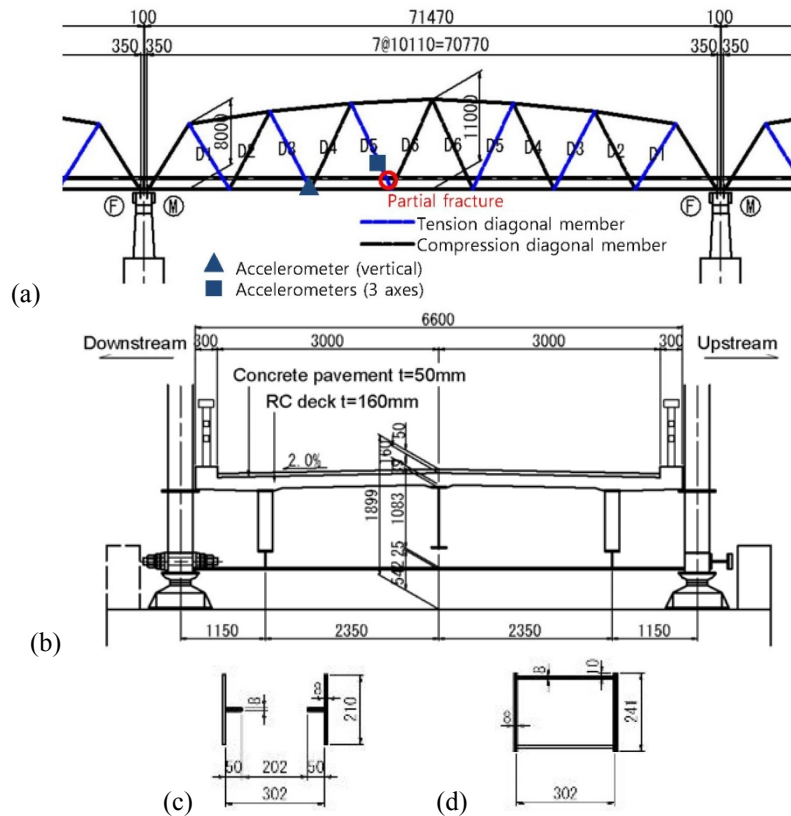


Fig. 1 Steel truss bridge investigated: (a) side view of single span (fourth span), (b) cross section of bridge, (c) cross section of tension diagonal member, (d) cross section of compression diagonal member. Unit [mm].



Fig. 2 (a) Partial fracture in D5 in fourth span and (b) repair with additional plates

Table 1 Comparison of modal properties of selected vibration modes between before and after repair

	Natural frequency [Hz]			Modal damping ratio		
	Before	After	Ratio	Before	After	Ratio
D5 in-plane only	7.146	9.847	-27%	0.0055 (0.0008)	0.0039 (0.0017)	41%
Lower chords	7.130	7.250	-2%	0.0106 (0.0005)	0.0059 (0.0003)	80%

There was limited time available for the measurement during the period of emergency repair work. Therefore, only five sensors were used in this measurement set. Accelerometers, ARF-10A or ARF-20A, Tokyo Sokki Kenkyujo, were attached to the diagonal member D5 at the upstream side at the quarter point of its length and to the lower chord members at both upstream and downstream sides at the quarter span. The measurement was made in the vertical, in-plane and out-of-plane directions at the diagonal member, and in the vertical direction only at the lower chord member. Signals from the accelerometers corresponding to vibrations including free vibration induced by the dump truck running were recorded in a laptop PC at 200 samples per second. The measurement duration was determined to cover free vibration lasting for about 30 seconds.

2.3 Experimental modal analysis

Modal properties of the bridge were identified from the field recorded data by the Eigensystem Realization Algorithm, ERA (Juang and Pappa 1985). Hankel matrices required at the first step in ERA were constructed from free vibration records extracted from the measured vibrations. The size of Hankel matrices was 1000 by 500, which was determined based on the stability of results in preliminary analyses. Raw results of the ERA analysis consisted of real modal properties and spurious modal properties due to measurement noise and other causes. In the present study, the screening criteria to extract realistic modes were the Modal Amplitude Coherence, MAC (Juang and Pappa 1985) calculated with all degrees of freedom used in the analysis, of 0.995 or greater and the damping ratio between 0 and 0.05. Stable poles in the stabilization diagram consisting of those satisfying the screening criteria were then extracted as real poles of the system.

2.4 Modal properties before and after repair in diagonal member

Fig. 3 shows examples of Fourier spectra of accelerations measured for a speed of 40 km/h with highest signal to noise ratio. The Fourier spectra were calculated with 8192 point FFT which resulted in the frequency resolution of 0.0244 Hz. As observed in Figs. 3(a) and (b), the dominant frequencies in the in-plane vibration of D5 were different before and after the repair. On the other hand, there were no clear changes in the vertical vibration of the lower chord (Figs. 3(c) and 3(d)).

Table 1 shows the results of the ERA analysis that were the averages and standard deviations determined from three repetitions of the dump truck running at 40 km/h. In the table, a set of modal properties identified from the ERA analysis with the data at D5 in-plane only, and another set identified with the data at two locations in the lower chords are presented. The details of those selected modes are discussed further with theoretical analysis in a later section of this paper.

For the modal properties obtained with D5 in-plane vibration only, the natural frequency decreased by 27% and the modal damping ratio increased by 41% with the partial fracture with respect to the structural condition after the repair on the assumption that the structural condition after the repair was close to its healthy condition (Table 1). For the modal properties identified from the vertical vibrations at the lower chords, the difference in natural frequency before and after the repair was not significant while the difference in modal damping ratio was 80%. The standard deviation of modal damping ratio shown in Table 1 was not large so that the average values identified could be considered reliable.

As observed in the table, the natural frequencies for the two modes before the repair were close together. It can be hypothesized that internal dynamic coupling between vibration of the main truss and vibration of the local diagonal member with the partial fracture could have occurred and caused the increases in the modal damping of the vibration mode identified from the records at the lower chord members. In order to discuss this possible mechanism of damping increase, more detailed modal analyses were conducted theoretically and experimentally.

3. Theoretical modal analysis of the truss bridge

3.1 Finite element models of the bridge

Three types of finite element, FE, models were developed with general-purpose FE software, FEMAP with NX Nastran V9.3 (Fig. 4). In order to understand the dynamic characteristics of the bridge, additional vibration measurements with fifteen sensors were conducted, as discussed later. The measurements were made at the first span of the bridge due to the limitation of measurement arrangement. The models were, therefore, developed based on the condition of the first span. In the first span, a partial fracture was found at the top of D5 diagonal member at downstream side, referred to as D5l, and additional plates were attached for repair (Fig. 4(b)).

Some details of the basic model in Fig. 4(a) are described below.

1) Any damages in the bridge, such as the corrossions in steel members and the deteriorations in the RC slab observed in the visual inspection, were not considered.

2) Each upper and lower chord member was modeled by a single beam element and each diagonal member was modeled by a single rod element with axial stiffness only.

3) The oval openings in the web of diagonal D3 and D5, shown in Fig. 2(a), were modeled by equivalent reduction in the cross sectional area distributed over the whole length of the member.

Table 2 Properties of cross section of D5 member with additional plates

	Cross sectional area		Moment of inertia of area	
	A [cm ²]	In-plane I_y [cm ⁴]	Out-of-plane I_z [cm ⁴]	
Healthy	41.6	123.5	9359	
With additional plates	214.2	5402	39707	
Ratio	5.1	4.4	4.2	

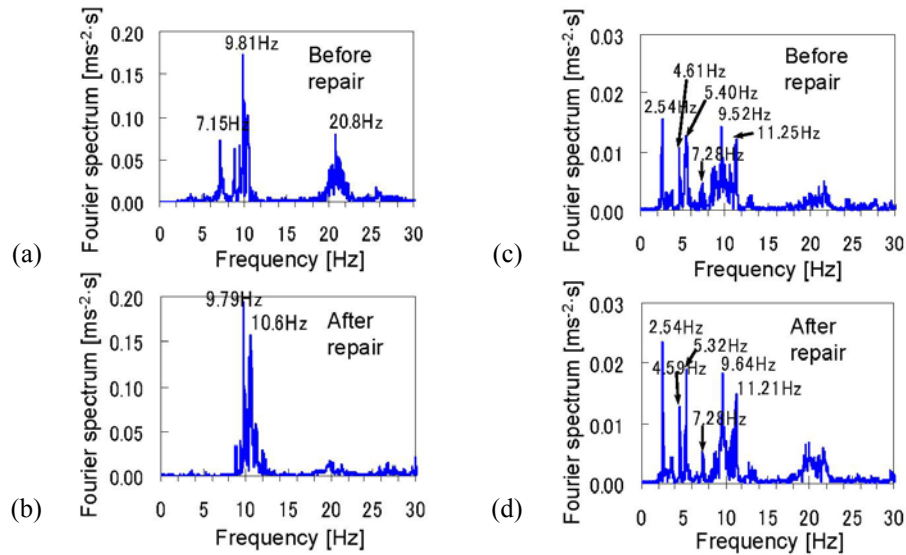


Fig. 3 Fourier spectra of measured acceleration. With dump truck running at 40 km/h. (a) D5, in plane, before repair, (b) D5, in-plane, after repair, (c) lower chord at quarter span, vertical, before repair, (d) lower chord at quarter span, vertical, after repair

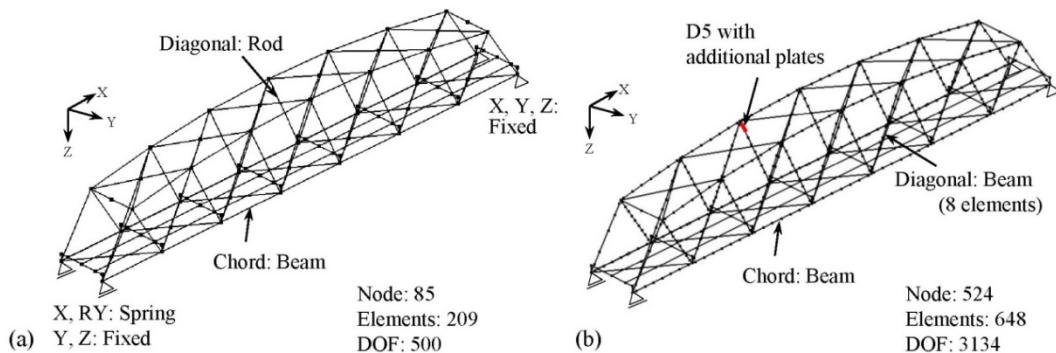


Fig. 4 (a) Basic model and (b) model with diagonal vibration and with additional plates

4) The contribution of the floor system and RC slab to the bending stiffness of the bridge was modeled by beam elements placed at the positions of stringers having stiffness equivalent to the stringers and the RC slab with Young's modulus ratio of 7. The cross beams, lateral bracings and portal bracings were modeled by beam elements.

5) For each beam element, the mass per unit length was assigned. The gusset plates attached to the diagonals and cross beams were modeled by lumped masses and assigned to the closest joint.

6) The Young's modulus and Poisson's ratio of steel were 2.0×10^8 kN/m² and 0.3, respectively.

7) It was reported that, in general, the horizontal displacements at roller supports and the rotational displacements at pin and roller supports are little in operational conditions and frictional forces act at those supports (Yoneda 1994). Therefore, the frictional resistance in the longitudinal translation at the roller supports and the rotation at the pin and roller supports were modeled by

spring elements. The spring constant for the longitudinal translation was determined as 1.0×10^4 kN/m that corresponded to the vertical reaction force of 1000 kN for self-weight, the dynamic friction coefficient of 0.01 and the longitudinal displacement of 1 mm. The spring constant for the rotation used in the analysis were 5.0×10^5 kNm/rad. These parameters were determined by trial and error based on the comparison with field vibration records, which is discussed in 4.3.2.

8) The piers and foundations were not modeled on the assumption that their effects on the operational vibrations of the superstructure were negligible.

The basic model described above neglected the vibration of diagonal members. In the model with diagonal vibration, the upper and lower chord and diagonal members were modeled by beam elements (Fig. 4(b)). The ends of diagonal members were modeled as rigid connections with the range of gusset plates in consideration, although the actual conditions could be elastic. In analyses with this model, the effect of self-weight was considered by conducting initial nonlinear static analysis and eigenvalue analyses were then conducted in consideration of the geometric stiffness. The effect of geometric stiffness appeared to be negligible for modal properties for global vibration modes of the bridge but increase the natural frequencies of local vibration modes dominated by vibration of tension diagonal member by about 10% (Yoshioka *et al.* 2009).

In addition, another model in consideration of additional steel plates at D5I for repair described above was developed. The effect of local structural change on the modal properties of the bridge could be understood theoretically from this model. Table 2 compares the properties of cross section of D5 in healthy and repaired conditions. These properties were assigned to the top element in D5I to model the increases in stiffness and mass by the additional plates (Fig. 4(b)).

3.2 Modal properties of the bridge

3.2.1 Classification of vibration mode

Table 3 shows the natural frequencies identified from the three models. In order to select vibration modes from different models for comparison, the Modal Assurance Criterion, referred to as MAC* in this paper, that indicated the similarity between different mode shapes were used.

$$MAC^* = \frac{|\phi \cdot \varphi|^2}{|\phi|^2 |\varphi|^2} \quad (1)$$

where ϕ and φ are modal vectors to be compared. A pair of vibration modes that yielded the maximum MAC* was selected for comparison in Table 3. The components in modal vectors for the degrees of freedom common in all models were used in the calculation of MAC*.

Fig. 5 shows principal vertical global modes identified in the model with diagonal vibration. In this paper, the vibration modes dominated by vibrations of the upper and lower chord members are called truss modes. There were vibration modes dominated by vibrations of diagonal members with no significant vibrations of the chord members, which are referred to as diagonal-dominant modes (Fig. 6). In the bridge studied, there were four diagonal members with common dimensions in a span, which resulted in four diagonal-dominant modes induced by those four diagonal members, such as those in Fig. 6 for D5. These four diagonal modes were different in the phases between the four diagonal members. Additionally, there were vibration modes in which vibrations of the main truss were coupled internally with local vibrations of diagonal members, as observed in Fig. 5. These vibration modes are referred to as diagonal-coupled modes in this paper. In such diagonal-coupled modes, deformations of the upper and lower chord members appeared to be relatively small due to significant deformations of diagonal members.

Table 3 Comparison of natural frequencies and MAC*

Mode shape	Basic		With diagonal vibration				With additional plates				
	Order	Freq. [Hz]	Order	Freq. [Hz]	(MAC*)	Ratio	Order	Freq. [Hz]	(MAC*)	Ratio	
1st horizontal symmetric	1	1.907	1	2.000	(0.90)	1.05	1	1.998	(0.91)	1.05	
1st vertical symmetric	3	2.446	2	2.567	(1.00)	1.05	2	2.567	(1.00)	1.05	
1st torsional symmetric	4	4.240	4	4.621	(0.85)	1.09	4	4.619	(0.83)	1.09	
Truss mode	1st vertical asymmetric	6	5.228	6	5.364	(1.00)	1.03	6	5.371	(1.00)	1.03
	1st horizontal asymmetric	7	5.333	7	5.600	(0.70)	1.05	7	5.599	(0.71)	1.05
	longitudinal rigid body	8	6.521	8	6.611	(1.00)	1.01	8	6.620	(1.00)	1.02
	2nd vertical symmetric	9	7.670	9	7.656	(0.83)	1.00	9	7.676	(0.83)	1.00
	1st torsional asymmetric	11	8.674	10	8.714	(0.97)	1.00	10	8.729	(0.97)	1.01
Coupled mode	2nd horizontal symmetric	12	8.879	11	8.956	(0.62)	1.01	11	8.958	(0.62)	1.01
Diagonal dominant mode (D5 in-plane)	1st (4 members in phase)	---	12	9.074	---	---	12	9.092	(0.73)	1.00	
	1st (up & downstream members out of phase)	---	13	9.135	---	---	13	9.186	(0.47)	1.01	
	1st (same side out of phase)	---	15	9.248	---	---	15	9.264	(0.48)	1.00	
	1st (4 members out of phase)	---	16	9.281	---	---	---	---	---	---	
	1st of D5 with additional plates	---	---	---	---	---	19	9.870	---	---	
Coupled mode	2nd vertical asymmetric	14	9.982	17	9.325	(0.91)	0.93	16	9.325	(0.90)	0.93
Truss mode	3rd vertical symmetric	15	11.272	21	9.990	(0.90)	0.89	21	9.992	(0.90)	0.89
Truss mode	2nd torsional symmetric	16	12.345	33	11.556	(0.80)	0.94	33	11.563	(0.81)	0.94

(The ratios and MAC* for truss and coupled modes were calculated with respect to the basic model.)

(The ratios and MAC* for diagonal modes were calculated with respect to the mode with diagonal vibration.)

(The 12th and 14th modes for the basic model were truss modes but, for comparison with other models, tabulated as coupled modes.)

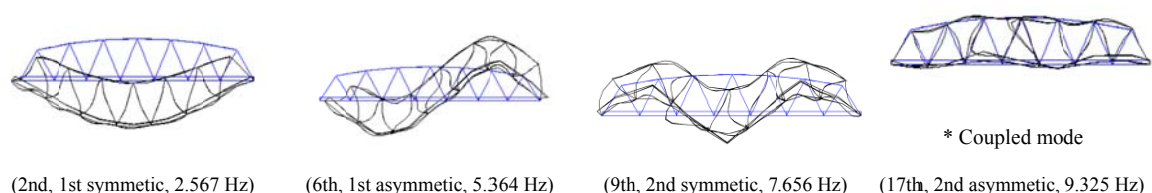


Fig. 5 Vertical truss modes (modal order, mode shape type, natural frequency)

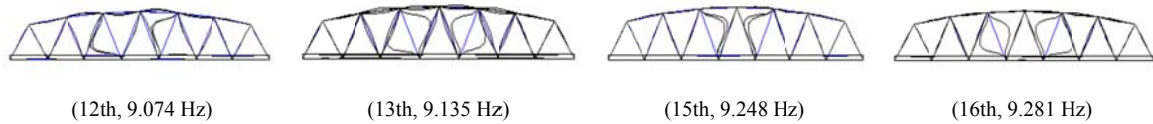


Fig. 6 Diagonal-dominant mode (modal order, natural frequency)

As discussed above, there were mainly three types of vibration modes, i.e., the truss, diagonal-dominant, and diagonal-coupled modes: the vibration modes identified from the models are classified into those three types in Table 3. It was, however, difficult to define general criteria to classify different types of vibration modes. In this study, therefore, those criteria were defined based on the ratio of the maximum component in modal vector for diagonal members to that of lower chord members for descriptive purposes: 0.6 or less for the truss mode, between 1.9 and 9.0 for the diagonal-coupled mode, and 12 or greater for the diagonal-dominant mode.

3.2.2 Distribution of natural frequencies and diagonal-coupled mode

Fig. 7 shows the distribution of natural frequencies, including those presented in Table 3, against modal order for the basic model and the model with diagonal vibration. For the basic model, there were truss modes only, as described above. As indicated in Fig 7, there were four diagonal-dominant modes at about 9 Hz for D5 members with the maximum slenderness ratio and, in addition, diagonal-coupled modes were observed also in that frequency range. This implies that dynamic coupling between a truss mode and a diagonal-dominant mode, resulting in a diagonal-coupled mode, could be induced when the natural frequencies of those modes were close together.

For the truss and diagonal-coupled modes at orders higher than the 2nd vertical asymmetric bending modes, the natural frequencies tended to decrease for the model with diagonal vibration, compared to the basic model, as observed in Table 3. These decreases in natural frequencies may be caused by increases in effective mass due to coupling of truss mode with diagonal-dominant mode. Additionally, the similarity of modal shapes between the basic model and the model with diagonal vibration tended to decrease by dynamic coupling between the main truss and the diagonal members, as observed in the decreases in the MAC* in Table 3.

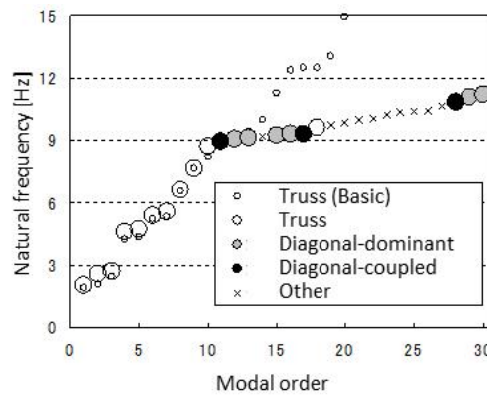


Fig. 7 Distribution of natural frequencies for basic model and model with diagonal vibration

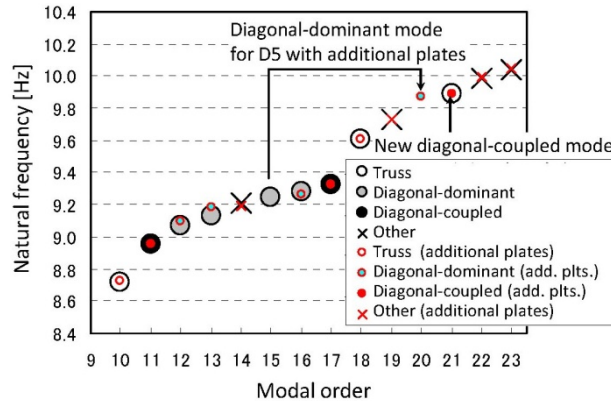


Fig. 8 Effect of additional plates on natural frequencies for 10th to 23rd modes

Effects of local structural change on modal properties are discussed by comparing results between the model with diagonal vibration and the model with additional plates. The natural frequency of the D5 dominant mode increased to 9.87 Hz for the mode with additional plates, although there were no other clear differences in natural frequencies between the two models (Table 3). This implies that the effects of additional plates on the natural frequencies of truss and diagonal-coupled modes were not significant. Fig. 8 compares the distribution of natural frequencies between the model with diagonal vibration and the model with additional plates for the 10th to 23th modes. A diagonal-coupled mode appeared at a frequency close to the natural frequency of diagonal mode of D5 with additional plates at 9.87 Hz.

4. Experimental identification of modal properties of the bridge

4.1 Vibration measurement

The modal properties identified theoretically in the previous section were compared with these obtained from a set of vibration measurement in the real bridge. The measurements were made at the first span where measurements with a wired system were possible. Fifteen vibration sensors consisting of 6 servo velocity-meters, VSE-15D, Tokyo Sokushin, and 9 piezoelectric accelerometers, PV-87, Rion, were located in two different arrangements (Fig. 9). Differences in the performance of two different sensors did not have any effects on the results in the frequency range between 2 and 20 Hz discussed in this paper. The velocity-meters used in the measurement had a capability of generating a signal proportional to acceleration. Accelerations of the bridge in service from all sensors were recorded at 100 samples per second for about 10 minutes.

The measurement locations in Case 1 shown in Fig. 9(a) were determined for the identification of global vibration modes of the main truss. Vertical vibrations were measured at locations on the road surface close to each node in the lower chord members except for both ends of the span where no measurable vertical vibration was expected. Additionally, vibrations were measured at the quarter point from the bottom of D5 at the upstream side, referred to as D5u. Two accelerometers located at the edges of the web measured in-plane vibration and an accelerometer

located at the center of the flange measured out-of-plane vibration as shown in Fig. 9(a).

In Case 2, accelerometers were placed at the quarter point of diagonal members, D5u, D5u', D5l, D5l' and D3l (Fig. 9(b)). Vertical vibrations at nodes in the lower chord members were also measured at the locations shown in Fig. 9(b). Additionally, vibrations in the horizontal direction perpendicular to the bridge axis were measured at the nodes U2 and U5 at the quarter span.

4.2 Experimental modal analysis

As in the preceding section, ERA was applied to free vibration records extracted from the measured vibration. Five and two free vibrations induced by a single vehicle passing, referred to as Vehicles 1 to 7, were selected from Cases 1 and 2, respectively, based on the vibration amplitude and video recording. The number of rows of Hankel matrices was 1500 times the number of sensors and the number of columns was 500, which were determined from preliminary analyses. In the analysis, the following screening criteria were used to extract realistic modal properties: the Modal Amplitude Coherence, MAC, of 0.9 or greater, the damping ratio between 0 and 0.05, the difference in the natural frequencies identified at two consecutive system orders of 0.02 Hz or less, and the Modal Assurance Criterion, MAC* defined in Eq. (1), of 0.9 or greater. In Eq. (1), ϕ and φ are the corresponding modal vectors identified at two consecutive system orders.

The measurement of in-plane motion of diagonal members included the effect of vertical and rotational motion of the main truss, which should be extracted so as to estimate the deformation of diagonal member only. The vertical and rotational rigid body displacements were calculated from the measurements at two adjacent joints in the lower chord and used to extract the effect of rigid body components from the in-plane measurement at diagonal members. In this adjustment, the horizontal displacement in the bridge axis was neglected, which could be justified by the fact that the horizontal displacement at roller support was little.

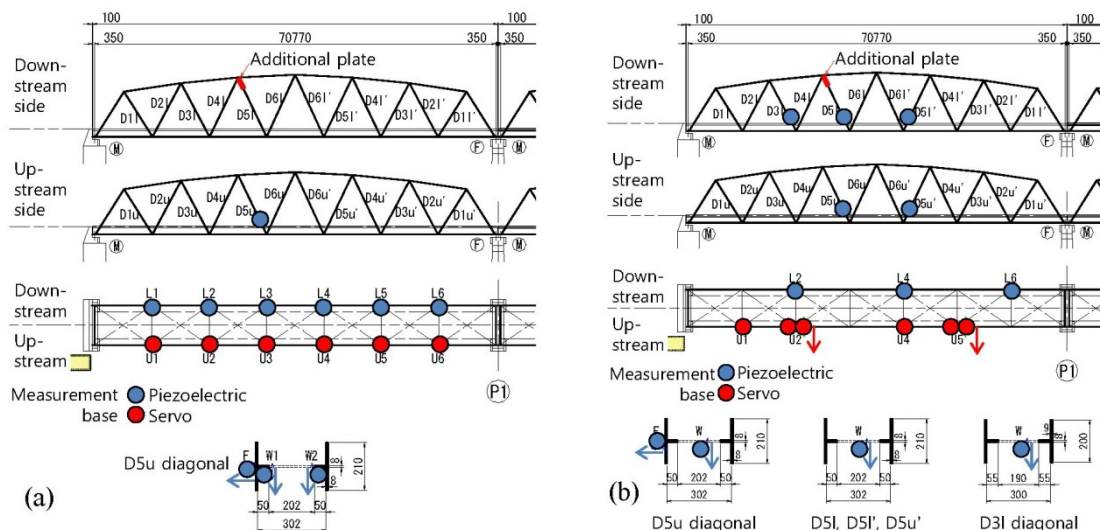


Fig. 9 Locations of vibration sensors. (a) Case 1, (b) Case 2

4.3 Modal properties identified experimentally

4.3.1 Modal properties identified from experiments

Fig. 10 shows a stabilization diagram obtained from the ERA analysis with 14 locations from Case 1. Fourteen channels out of 15 were used in the analysis because, in Case 1, the measurement at the joint U3 was not properly recorded. In Fig. 10, the Fourier spectra of the accelerations at U1 are also shown. In the frequency range below 8 Hz, the natural frequencies identified stably by ERA agreed with the peak frequencies in the Fourier spectra. On the other hand, there were many natural frequencies identified by ERA at frequencies around 9 Hz, although one peak only was observed in the acceleration spectra at U1, which implies that there were many diagonal dominant modes in this frequency range. Additionally, the natural frequencies identified from the model with additional plates in the FE analysis are presented at the top of Fig. 10. Although there was a difference between the natural frequency of 7.676 Hz in the analysis for the 2nd vertical symmetric mode and the corresponding experimental value, the analytical and experimental values agreed well for lower order modes than that mode.

4.3.2 Discussion of experimentally identified modal properties

Table 4 compares the natural frequencies identified from the experiments and the FE model. The variations in the natural frequencies with different vehicles were not significant although the variations for the 1st vertical symmetric, 2nd vertical asymmetric, and 2nd torsional symmetric modes were relatively greater than the other modes. In Table 4, the values in brackets are the MAC* calculated with the components in modal vectors for the joints in the lower chords normalized by the maximum vertical component for the lower chords.

For lower order modes from the 1st vertical symmetric to the 1st vertical asymmetric modes, the differences in natural frequencies between experiment and analysis were less than 1% and the MAC* ranged between 0.99 and 1. It should be noted that the theoretical results were obtained with support conditions that modeled support friction by spring constants determined by trial and error within a range physically reasonable. If the frictions at the supports were neglected, the natural frequency of the 1st vertical symmetric mode differed from the experimental identification by -6%. The effect of support friction was clear in the 1st vertical symmetric and 1st vertical asymmetric modes only.

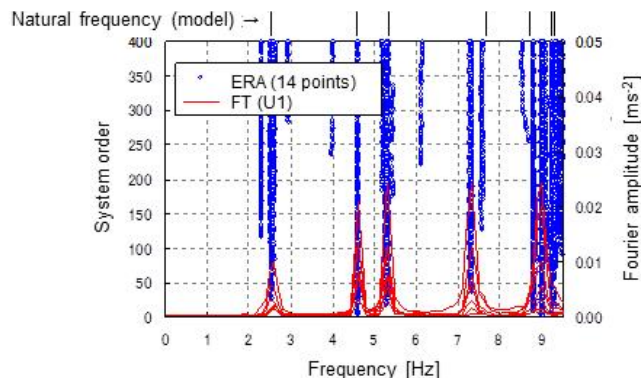


Fig. 10 Natural frequencies from experiment (ERA and FT) and FE model (Vehicles 1 to 7)

Table 4 Comparison of natural frequencies (in [Hz]) between experiment and theoretical analysis

Mode shape	Experiment								Analysis (MAC*)	Ord. Frq.	Ratio Ex/An	
	Case 1				Case 2							Average
	Veh. 1	Veh. 2	Veh. 3	Veh. 4	Veh. 5	Veh. 6	Veh. 7					
	(Dump)	(1 box)	(Coupe)	(Truck)	(Truck)	(Coupe)	(Coupe)					
1st horizontal symmetric	---	---	---	---	---	---	---	---	(--)	1	1.998	---
1st vertical symmetric	2.570	2.531	2.541	2.552	2.544	2.587	2.587	2.559	(1.00)	2	2.567	1.00
1st torsional symmetric	4.605	4.609	4.606	4.617	4.603	4.610	4.608	4.608	(1.00)	4	4.619	1.00
Truss 1st vertical asymmetric	5.293	5.302	5.324	5.239	5.302	5.305	5.302	5.295	(0.99)	6	5.371	1.01
longitudinal rigid body	---	---	6.133	---	---	---	---	6.133	(0.73)	8	6.620	1.08
2nd vertical symmetric	7.300	7.316	7.309	7.305	7.306	---	7.308	7.307	(0.98)	9	7.676	1.05
1st torsional asymmetric	---	8.810	8.815	8.816	---	8.822	---	8.816	(0.80)	10	8.729	0.99
Diagonal 4 members in phase	9.006	9.008	9.007	9.005	9.008	9.021	9.025	9.011	(--)	12	9.092	1.01
(D5) Opposite side out of phase	9.052	9.325	9.243	9.339	9.243	9.090	---	9.215	(--)	13	9.186	1.00
in-plane) Same side out of phase	9.241	---	9.358	---	---	9.101	---	9.233	(--)	15	9.264	1.00
1st with additional plates	---	---	---	---	---	9.762	9.932	9.847	(--)	19	9.870	1.00
Coupled 2nd vertical asymmetric	9.240	---	---	---	9.320	9.338	9.290	9.297	(0.74)	16	9.325	1.00
Truss 3rd vertical symmetric	10.169	10.076	---	10.123	10.099	10.121	10.132	10.120	(0.88)	21	9.992	0.99
2nd torsional symmetric	11.548	11.674	11.240	11.356	11.792	11.390	11.388	11.484	(0.91)	33	11.563	1.01

(For the calculation of MAC*, components in modal vector for diagonal members were not used.)
 (For diagonal-dominant modes, the modal shapes could not be identified due to limited number of sensors.)

The difference in natural frequency for the longitudinal rigid body mode between experiment and analysis was 8% with the MAC* of 0.73. These differences in natural frequency and mode shape may be because the spring constants determined to reduce differences between experiment and analysis mainly for lower order modes were not appropriate for the longitudinal rigid body mode. The longitudinal rigid body mode identified with Vehicle 3 only may be difficult to be induced by vehicle passing and cannot be judged as an effective mode for health monitoring. Therefore, the spring constants for the support were not updated to represent this mode.

For the 2nd vertical symmetric mode, the MAC* was relatively high at 0.98 but the differences in natural frequency was 5%. This difference in natural frequency might be caused by possible error in the spring constants representing support friction. The MAC* was relatively high possibly because the horizontal components in modal vectors were not used.

For higher order modes than the 1st torsional asymmetric mode with complex mode shapes, the MAC* was not high but the natural frequencies identified from experiment and theoretical analysis agreed well with a difference of about 1%.

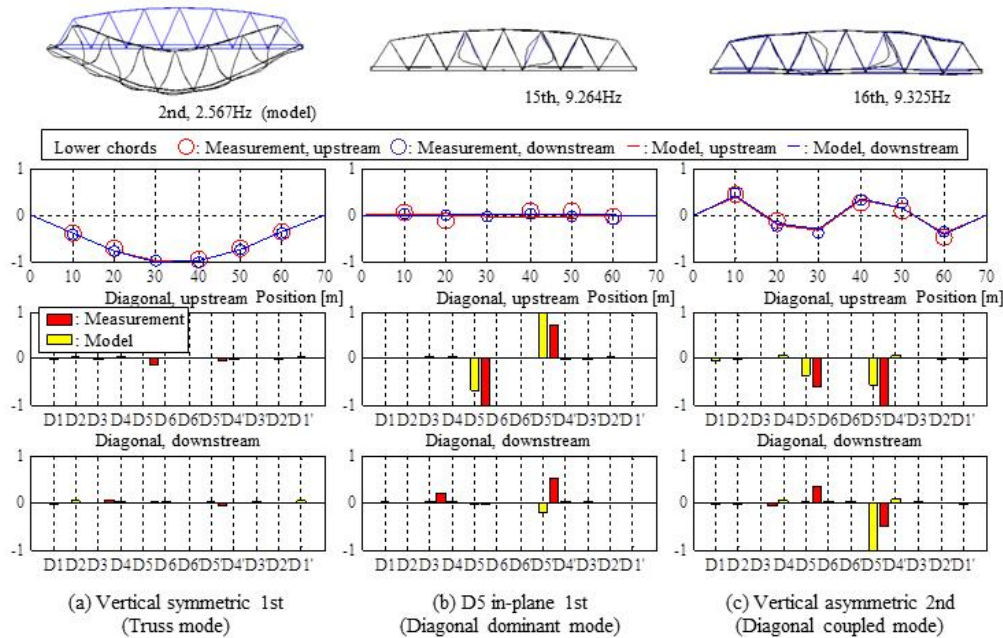


Fig. 11 Comparison of mode shapes identified from experiment and model

The D5 diagonal dominant modes in the experiment appeared to correspond to those identified theoretically, although the modal shapes were not identified clearly. For the Case 1, the four vibration modes dominated by D5 motion were identified at frequencies around 9 Hz but their mode shapes could not be distinguished with the measurement at a single D5 member only. For the Case 2, the measurement was made at four D5 diagonals but the corresponding measurements at the joints in the lower chords could not be made so that the adjustment to estimate the amplitude of diagonal members only was not possible.

4.3.3 Dynamic coupling of diagonal members

In order to investigate the internal dynamic coupling between the main truss and diagonal members, the normalized modal vectors identified from Cases 1 and 2 were combined. The modal vectors identified from Vehicle 1 in Case 1 were combined with those from Vehicle 6 in Case 2 based on the closeness of natural frequencies. The components in modal vectors common in the two measurement cases were averaged in the combination.

Examples of the mode shapes are compared with the corresponding mode shapes obtained with the model with additional plates in Fig. 11. The top figures are the mode shapes in the FE analysis, the figures in the second row are the mode shapes for the lower chord members in the experiment and the FE analysis, and the figures at bottom two rows show the components in modal vectors for diagonal members after the adjustment described above by bar plot. The components of modal vectors shown in Fig. 11 were normalized by the maximum component in modal vector among all measurement locations. As observed in Figs. 11(a) and 11(b), the truss and diagonal-dominant

modes obtained theoretically were identified in the experiment, although there were some discrepancies in components in modal vectors. The modal component of D5 at downstream side appeared to be small in the experiment and analysis. The 2nd vertical asymmetric mode appeared to be coupled with vibration of D5 with similar trends in modal vector in the experiment and analysis (Fig. 11(c)).

Fig. 12 shows the degree of coupling of vibration of D5u diagonal member with vibration of the main truss represented by the ratio of the component in modal vector for D5u to the maximum component in modal vector for the lower chords. Although there appeared to be discrepancies between the experiment and theoretical analysis, increases in the degree of coupling were observed in the frequency range 9 to 11 Hz for the experiment and analysis. Possible reasons for discrepancies in the degree of coupling between experiment and analysis may include the fixed ends of diagonal members in the model that might not represent possible loosening of rivets. Particularly, if this coupling was interpreted as internal resonance, the effect of damping at connections on resonance responses would be significant. There were diagonal-dominant modes induced by Vehicles 1 and 2 observed at about 10.7 Hz that were not identified in the theoretical analysis. An additional FE analysis showed that these diagonal dominant modes could be torsional modes of diagonal member, although the details of analysis are not presented in this paper.

4.3.4 Dependence of modal damping on amplitude

Fig. 13 shows the relation between modal damping ratios and natural frequencies identified by ERA with Vehicles 1 to 7. As observed in Fig. 13, there were variations in the modal damping ratios identified after the screening described in the preceding section. The modal damping ratios for the 1st vertical symmetric and 1st vertical asymmetric modes varied with different vehicles. For other modes, the variations in modal damping ratios appeared to be small, although those modes were identified from less number of records.

A possible source of the variation in modal damping ratios for the lower order modes might include the dependence of modal damping on vibration amplitude. Fig. 14 shows the relation between modal damping ratios and the maximum initial modal amplitude in the lower chords for Vehicles 1 to 7. The initial modal amplitude was determined by dividing the initial modal acceleration amplitude identified by ERA by the square of natural circular frequency. All modal damping ratios identified stably at different system orders were shown in the figure.

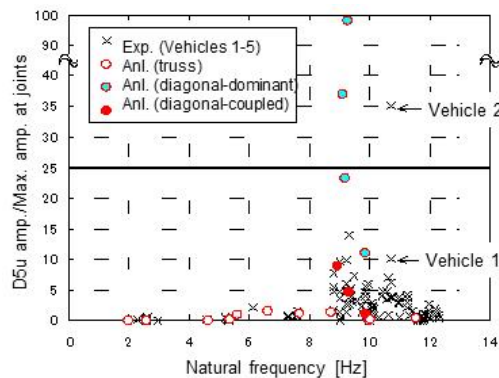


Fig. 12 Degree of coupling of D5u diagonal member with main truss

The modal damping ratios for the lower order modes in Fig. 14(a), in particular the 1st vertical symmetric mode, showed amplitude dependence in which the modal damping ratio tended to increase with increases in the initial modal amplitude. In a separate study, theoretical complex modal analysis was conducted with frictional damping at the movable supports and material damping in members, and the results showed that the contribution of the frictional damping to modal damping appeared to be significant in those lower order modes (Yoshioka *et al.* 2009). According to those results, the amplitude dependence of modal damping for the lower order modes may be caused by amplitude dependence of frictional damping at the supports.

For other higher order vertical modes including the 2nd vertical asymmetric mode, which was a diagonal-coupled mode, there were no clear signs of amplitude dependence in modal damping ratio, although these modes were identified in a range of small amplitude only. This may imply that, for higher order vertical modes that can be coupled with local vibration of diagonal members, the modal damping ratio can be identified stably and, therefore, those modes could be used to detect possible changes in damping due to damages in diagonal members.

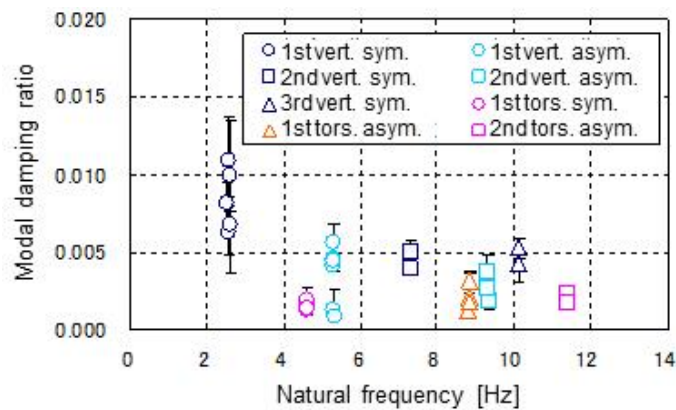


Fig. 13 Relation between modal damping ratios and natural frequencies identified experimentally

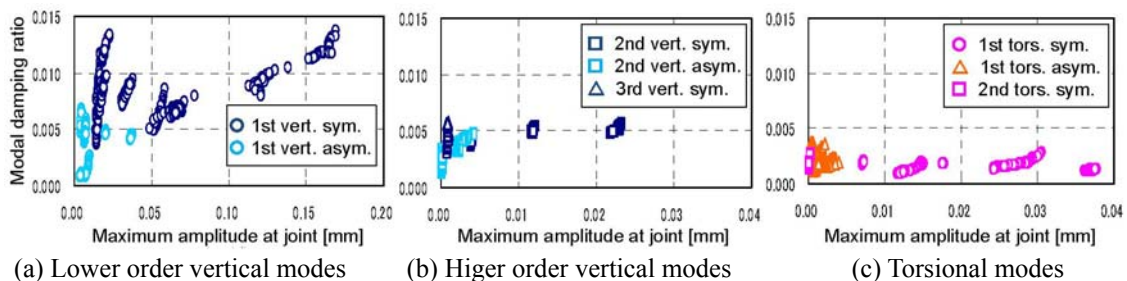


Fig. 14 Amplitude dependence of modal damping ratios. sym: symmetric; asym.: asymmetric

5. Detection of damages in diagonal members based on changes in modal damping

As discussed in 2.4, changes in modal properties were observed before and after the repair in the diagonal member. There were significant changes in modal damping ratio for the vibration modes shown in Table 1. Comparisons between the Fourier spectra shown in Fig. 3 and the results of theoretical and experimental modal analysis could conclude that the mode with D5 in-plane only was the 1st in-plane symmetric bending mode of the diagonal member, and the mode with the lower chords was the 2nd vertical symmetric mode that was coupled with vibration of D5 members (Table 1). This implies that diagonal-coupled modes that can be identified with small number of sensors at joints in lower chords could be used to detect damages in diagonal members.

In order to understand coupling between the 2nd vertical symmetric mode and diagonal-dominant mode for D5 with the partial fracture, an additional ERA analysis was conducted with data measured with one sensor at D5 and two at the lower chords. Fig. 15 shows the relation between natural frequency and modal damping ratio for the diagonal-dominant mode and the 2nd vertical symmetric mode, and the relation between natural frequency and degree of dynamic coupling of D5 with the main truss. The degree of dynamic coupling was defined by dividing the component in modal vector for D5 by that at the lower chord. For the 2nd vertical asymmetric mode, although no significant coupling of D5 with the main truss was observed after the repair, D5 diagonal before the repair was coupled clearly due to decrease in natural frequency of diagonal-dominant mode. The coupling of D5 with the main truss caused an increase in modal damping of the 2nd vertical symmetric mode possibly due to damping increase in the damaged diagonal.

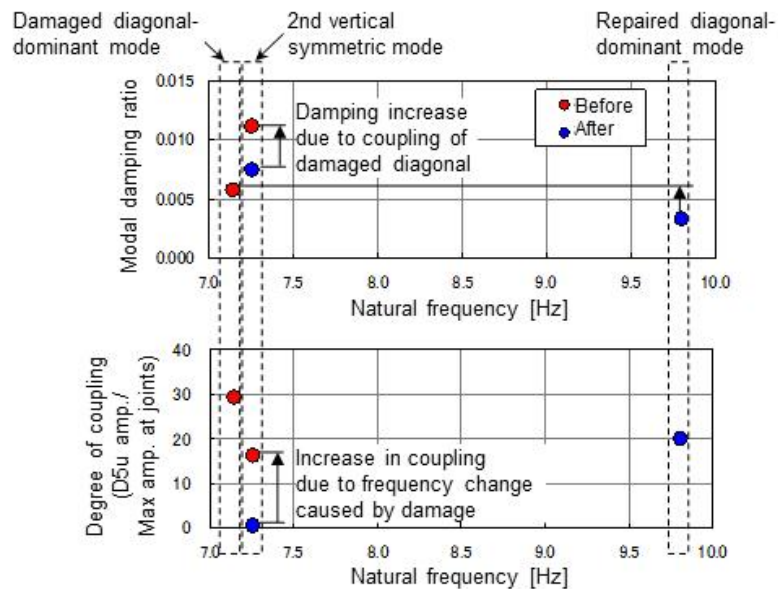


Fig. 15 Changes in modal properties of 2nd vertical symmetric mode before and after repair

The discussion above implies that modal damping ratios of diagonal-coupled modes could be used to identify damages in diagonal members: damages in diagonal members could be detected without direct measurement of vibrations of diagonal members, which could lead to an effective SHM based on vibration measurement. For bowstring type truss bridges, such as the bridge investigated in this study, the natural frequencies of diagonal-dominant modes are different depending on the length of diagonal members so that it could be possible to identify members with damage by the method discussed here.

It should be noted that damages discussed in this paper were cracks that could induce significant increase in frictional damping. Further investigations are required to identify types of damages which could be detected by the method discussed in this study.

6. Conclusions

Conclusions derived from this study are listed below.

- Vibration modes of truss bridges include truss modes that are vibration of the main truss with vibration of the upper and lower chord members dominant, diagonal-dominant modes that are local vibration mode, and diagonal-coupled modes in which truss mode and diagonal-dominant mode are coupled together.
- A local structural change, i.e., the repair of damaged diagonal member with additional steel plates in this study, did not have significant effect on the natural frequency of diagonal-coupled mode, but caused relatively clear changes in the degree of coupling between diagonal member and main truss. Although quantitative evaluation of the degree of coupling was difficult, there was qualitative consistency between the experiment and theoretical analysis.
- The modal damping ratios identified experimentally showed clear variations. Amplitude dependence of modal damping was observed for the 1st vertical symmetric mode and 1st vertical asymmetric mode with significant effect of frictional damping at the supports. However, for higher order vibration modes that could be coupled with local diagonal vibration, the modal damping ratios could be identified stably and their dependence on amplitude was not significant. These can be advantages in evaluating the condition of diagonal members based on damping changes in diagonal-coupled modes.
- The experimental modal analysis with vibration records measured in the bridge before and after the repair of damaged diagonal member showed little changes in natural frequencies but clear increases in modal damping ratio possibly due to coupling of damaged diagonal member. This implies that damages in diagonal members could be detected by monitoring damping of diagonal-coupled modes with a small number of sensors.

References

- Balageas, D., Fritzen, C.P. and Guemes, A. (2006), *Structural Health Monitoring*, Wiley-ISTE
- Boller, C., Chang, F.K. and Fujino, Y. (2009), *Encyclopedia of Structural Health Monitoring*. Wiley.
- Doebling, S.W., Farrar, C.R., Prime, M.B. and Shevitz, D.W. (1996), *Damage identification and health monitoring of structural and mechanical systems from changes in their vibration characteristics*, A Literature Review, Los Alamos National Laboratory Report La-13070-MS.

- Fujino, Y. and Siringoringo, D.M. (2008), "Structural health monitoring of bridges in Japan: an overview of the current trend", Proceedings of the *4th International Conference on FRP Composites in Civil Engineering*, Zurich.
- Juang, J.N. and Pappa, R.S. (1985), "An eigensystem realization algorithm for modal parameter identification and modal reduction", *J. Guid. Control. Dynam.*, **8**(5), 620-627.
- Kim, J. and Stubbs, N. (2003), "Nondestructive crack detection algorithm for full-scale bridges", *J. Struct. Eng.- ASCE*, **129**(10), 1358-1366.
- Ko, J.M. and Ni Y.Q. (2005), "Technology developments in structural health monitoring of large-scale bridges", *Eng. Struct.*, **27**, 1715-1725.
- Maeck J. and de Roeck, G. (2003), "Damage assessment using vibration analysis on the Z24-bridge", *Mech. Syst. Signal. Pr.*, **17**(1), 133-142.
- National Guideline (2014), *Guideline for periodic inspection of bridges*, Ministry of Land, Infrastructure, Transport and Tourism, Japan. (in Japanese)
- Shama, A.A., Mander, J.B., Chen, S.S. and Aref, A.J. (2001), "Ambient vibration and seismic evaluation of cantilever truss bridge", *Eng. Struct.*, **23**, 1281-1292.
- Spyrakos, C.C., Raftoyiannis, I.G. and Ermopoulos, J.C. (2004), "Condition assessment and retrofit of a historic steel-truss railway bridge", *J. Constr. Steel Res.*, **60**, 1213-1225.
- Yamaguchi, H., Fujiwara, T., Yamaguchi, K., Matsumoto, Y. and Tsutsumi, K. (2004), "Coupling of cable vibration and its damping effect in long span cable-stayed bridge: the Tatara Bridge", *J. Struct. Mech. Earth. Eng. - JSCE*, **766**(68), 309-323. (in Japanese)
- Yoneda, M. (1994), "Some considerations on damping characteristics of bridge structures due to Coulomb friction force at movable support", *J. Struct. Mech. Earth. Eng. - JSCE*, **492**/I-23, 137-145. (in Japanese).
- Yoshioka, T., Yamaguchi, H., Ito, S. and Harada, M. (2009), "Identification vibration characteristics of the steel truss bridge and influence of diagonal member damage on damping", *Kozo Kogaku Ronbunshu, A (J. Struct. Eng., A)*, **60A**, 295-305. (in Japanese)